[6]Baker, D. N., Akasofu, S.-I., Baumjohann, W., Bieber, J. W., Fairfield, D. H., Hones, E. W., Jr., Mauk, B., McPherron, R. L., and Moore, T. E., "Substorms in the Magnetosphere, Solar Terrestrial Physics: Present and Future," *NASA Ref. Publ.*, pp. 1120-1128, Chap. 8, 1984.

[7]Kremser, G., Korth, A., Ullaland, S. L., Perraut, S., Roux, A., Pedersen, A., Schmidt, R., and Tanskanen, P., "Field-Aligned Beams of Energetic Electrons (16 keV $\leq E \leq$80 keV) Observed at Geosynchronous Orbit at Substorm Onsets," *Journal of Geophysical Research*, Vol. 93, No. A12, 1988, pp. 14,453-14,464.

[8]Roux, A., Perraut, S., Robert, P., Morane, A., Pedersen, A., Korth, A., Kremser, G., Aparicio, B., Rodgers, D., and Pellinen, R., "Plasmasheet Instability Related to the Westward Travelling Surge," *Journal of Geophysical Research*, Vol. 96, No. A10, 1991, pp. 17,697-17,714.

[9]Korth, A., Kremser, G., Cornilleau-Wehrlin, N., and Solomon, J., "Observations of Energetic Electrons and VLF Waves at Geostationary Orbit During Storm Sudden Commencements (SSC)," *Solar Wind-Magnetosphere Coupling*, edited by Y. Kamide and J. A. Slavin, Terra Scientific Publishing Co., Tokyo, Japan, 1986, pp. 391-399.

[10]Wilken, B., Baker, D. N., Higbie, P. R., Fritz, T. A., Olsen, W. P., and Pfitzer, K. A., "Magnetospheric Configuration and Energetic Particle Effects Associated with a SSC: A Case Study of the CDAW 6 Event on March 22, 1979," *Journal of Geophysical Research*, Vol. 91, No. A2, 1986, pp. 1459-1473.

[11]Ullaland, S. L., Kremser, G., Tanskanen, P., Korth, A., Torkar, K., Block, L., and Iversen, I. B., "Influence of a Storm Sudden Commencement on the Development of a Magnetospheric Substorm: Ground, Balloon, and Satellite Observations," *Journal of Geophysical Research*, (submitted for publication), 1992.

[12]Koga, R., Imamoto, S. S., Katz, N., Pinkerton, S. D., "Data Processing Units for Eight Magnetospheric Particle and Field Sensors," *Journal of Spacecraft and Rockets*, Vol. 29, No. 4, 1992, pp. 574-579.

CRRES Spectrometer for Electrons and Protons

R. W. Nightingale,* R. R. Vondrak,† E. E. Gaines,* W. L. Imhof,‡ R. M. Robinson,§ S. J. Battel,¶ D. A. Simpson,** and J. B. Reagan††
Lockheed Palo Alto Research Laboratory, Palo Alto, California 94304

Introduction

IMPORTANT components of the magnetospheric plasma to be explored by the CRRES are the energetic electrons and protons that populate the Earth's radiation belts. The fluxes of these particles depend critically on the production and loss mechanisms in the radiation belts and exhibit dynamic behavior in response to solar and geomagnetic activity.[1,2] The understanding of these processes requires detailed measurements of the particle distribution functions including the pitch angle. Previous measurements of energetic electrons and protons have been made by instruments on satellites such as Ogo 5,[3] SCATHA,[4] (S/C) 1979-053, and (S/C) 1982-019,[1,2] but the unique CRRES orbit offers exciting new possibilities for developing improved models of the inner and outer radiation belts.[5,6] For example, the particle distributions measured along the spacecraft trajectory can be used to map the two-dimensional radiation belt morphology in the orbit plane for $1.05 < L \leq 7$ near the geomagnetic equator.

The ONR 307-3 Spectrometer for Electrons and Protons (SEP) is one component of the ONR 307 Energetic Particles and Ion Composition experiment. SEP measures the energy and pitch angle distributions of energetic electrons and protons throughout the CRRES orbit. The specific science objectives of the SEP experiment are 1) to understand the physics of the sources, losses, energization, transport, and lifetimes of energetic particles in the Earth's radiation belts; 2) to understand the details of wave-particle interactions (WPI), both natural and man made, that result in precipitation of radiation belt particles; and 3) to utilize this experimental data base to greatly improve the accuracy of trapped radiation belt models.

Experiment Description and Operations

The SEP design is based heavily on the successful SC-3 spectrometer[4,7] flown on the SCATHA mission. Unlike the single-detector system used on SCATHA, SEP consists of three solid-state particle spectrometers oriented at 40, 60, and 80 deg from the spacecraft spin axis. A cross-sectional view of one of the telescopes is shown in Fig. 1. Each spectrometer has four detector elements labeled A, D, E, and E′. Various logic combinations of the four detector elements in each spectrometer are used to determine the particle types and energy ranges, which are measured sequentially. The operational modes of each telescope are individually commandable.

The D detector, which is 200-μm-thick intrinsic silicon, is used to measure both the rate of energy loss of the higher-energy particles and to directly stop and measure the low-energy particles. The E detector, which consists of a stack of five 2-mm-thick silicon surface-barrier detectors in parallel, is located behind the D detector to stop the higher-energy particles and to measure their total energy loss. The E′ detector, which is a 1000-μm-thick piece of silicon, is located behind the E detector and is used as an active collimator. Following it is a tungsten absorber that sets the upper energy limit for analysis. The entire telescope-configured stack is surrounded by the anticoincidence A detector, which consists of a plastic scintillator viewed by a photomultiplier tube. The A detector senses and rejects energetic particles and bremsstrahlung that penetrate either the outer shielding walls of aluminum and tungsten or the silicon detector stack and tungsten absorber. The detector stack is located behind a long, narrow collimator that defines the 3-deg angular field of view full width at half maximum (FWHM). The aluminum and tungsten effectively stop electrons with energy up to 5 MeV and bremsstrahlung photons with energy up to about 150 keV.

Each of the three identical SEP particle telescopes has a high-resolution, 3-deg (FWHM) field of view provided by a long collimator (20 cm) containing 10 baffles. The collimators are identical to the ones used on the SC-3 instrument,[4] providing an instrument geometric factor of $\sim 3 \times 10^{-3}$ cm^2-sr. For the 80- and 60-deg telescopes, measurements over 12 energy channels are obtained every 0.25 s with a dead time of 2 ms. Because of telemetry restrictions, the 40-deg telescope accumulates for 0.5 s with a dead time of 4 ms.

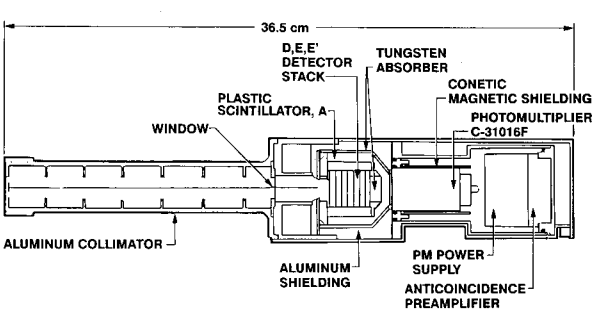

Fig. 1 Cross-sectional view of one of the SEP telescopes.

Received June 18, 1991; revision received Sept. 3, 1991; accepted for publication Sept. 3, 1991.

*Research Scientist.
†Manager. Associate Fellow AIAA.
‡Consulting Scientist.
§Staff Scientist.
¶Consultant, Battel Engineering. Member AIAA.
**Senior Staff Research Engineer.
††General Manager. Fellow AIAA.

The three SEP spectrometer heads and the analyzer package are shown in Fig. 2. The two units are mounted on the bottom of the spacecraft and are separated to achieve a lower temperature in the silicon detectors for improved low-energy electron detection.[8,9]

Each sensor operates from its own 256, 8-bit word CMOS memory, which is individually addressable and loadable via a 16-bit serial-digital command. Four of these words completely define one operating mode (32-bit control register) for an individual sensor. A mode is defined by specifying the logic conditions (coincidence/anticoincidence), gain, detector for pulse-height analysis, and energy thresholds required between the four detector elements to uniquely establish a particular type and energy range for analysis.[4]

Several modes can be programmed in sequence to emphasize one particle type, to obtain comprehensive measurements for special events such as solar flares, or to dwell on a narrow energy range for any particle type. A hard-wired backup mode that measures the higher-energy electrons (215–5100 keV) is independent of the memory and is used automatically at turn-on and whenever the memory is being loaded or disabled. The basic programmable mode parameters are the energy range and energy channel widths for the electrons and for the protons. Typical modes that may be used during the CRRES mission are shown in Table 1.

Calibration

The SEP sensor heads were calibrated using electron and proton beams from accelerators at the Goddard Space Flight Center (GSFC) in Greenbelt, Maryland, and at Harvard University in Cambridge, Massachusetts. Two accelerators were utilized at GSFC, a low-energy electron machine for energies up to 150 keV and a Van de Graaff accelerator with a maximum energy of 1.5 MeV for both electrons and protons. The sensors were in vacuum at room temperature for these runs. The beam rate of the low-energy accelerator was stable to about 25% at a few thousand counts per second for electrons between 25 and 150 keV. The Van de Graaff accelerator extended the electron measurements to 1500 keV in 10 steps and started the proton range from 500 to 1500 keV in five energy steps.

High-energy proton calibrations were done in air at the Harvard Cyclotron Laboratory for eight energy steps between 35 and 100 MeV. The 159-MeV proton beam was reduced in energy by absorbers that produce a beam energy spread of less than 6% at 90 MeV and above, whereas the spread is about 40% at the lowest energies. The measured energy deposition from higher-energy protons penetrating the detectors was within 1 MeV of calculated values.

Figure 3 shows examples of calibration data for electrons and protons. The spectra of monoenergetic beams were obtained with a laboratory multichannel analyzer and were related to the 12 channels of the flight pulse-height analyzers by voltage levels. The calibration data were used to specify the energy ranges for each mode of each sensor as shown in Table 1. The mode ranges are electronically divided into 12 channels, each approximately having the channel width shown in the table. The energy ranges in Table 1 show some overlap between modes. The particle collimation, the D detector absorption, and the sensor coincidence circuitry combine to significantly reduce the overlap.

Results

SEP commenced normal operations on August 7, 1990, after a successful instrument activation period. Preliminary results are shown in Figs. 4 and 5. Figure 4 shows pitch angle spectrograms for electrons and protons measured during orbit 79 by the sensor that is 80 deg from the spin axis. This orbit occurred several days after the commencement of a moderate magnetic storm (Dst = − 116). Each panel shows the relative flux of electrons or protons integrated over the energy ranges

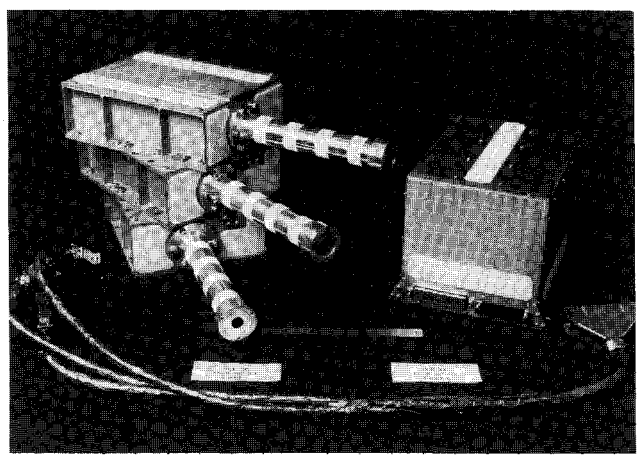

Fig. 2 Photograph of the three SEP telescopes mounted together and the electronics analyzer package.

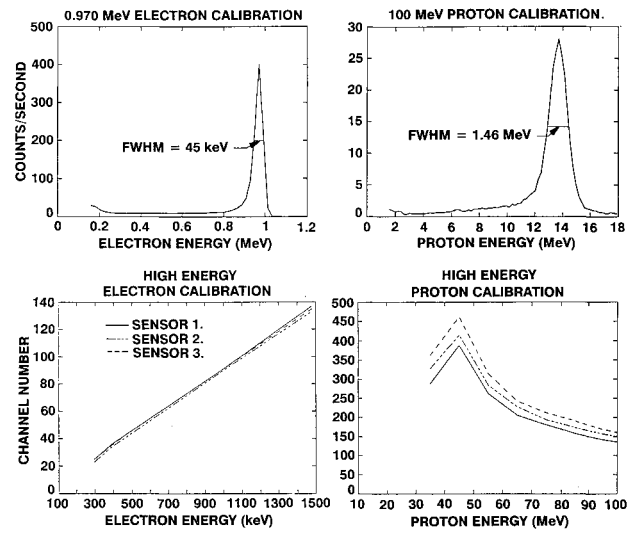

Fig. 3 Examples of calibration data showing typical spectra of the particle beams and the pulse-height responses vs energy in all three sensors for high-energy electrons and protons.

Table 1 SEP initial energy range and channel width

	Sensor A		Sensor B		Sensor C	
Mode	Energy range, MeV	Width, MeV	Energy range, MeV	Width, MeV	Energy range, MeV	Width, MeV
Electron 1	0.042–0.324	0.0235	0.042–0.336	0.0245	0.041–0.313	0.0227
Electron 2	0.164–4.93	0.397	0.171–5.12	0.413	0.170–5.11	0.412
Proton 1	0.875–6.60	0.478	0.916–6.70	0.482	0.920–6.80	0.490
Proton 2	2.5–38.7	3.01	2.2–33.7	2.62	2.0–30.4	2.37
Proton 3	35.8–80.2	3.7	31.2–69.9	3.22	28.2–63.1	2.91
Proton 4	45–94	4.08	45–105	5.00	45–110	5.42
Alphas	6.8–24	1.43	6.90–24.3	1.45	7.00–24.	1.47

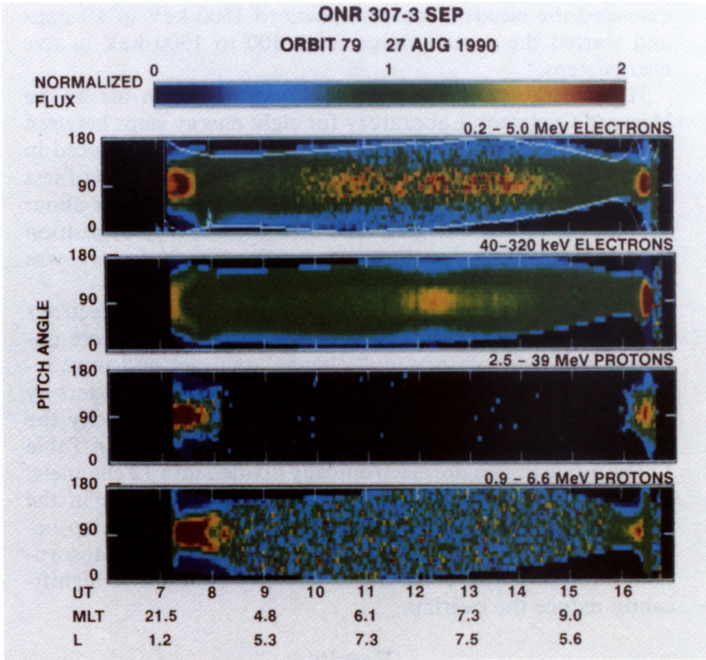

Fig. 4 Pitch angle spectrograms showing relative intensities of electrons and protons measured during orbit 79. The intensities are normalized to the average differential, directional flux measured during the 64-s sampling interval.

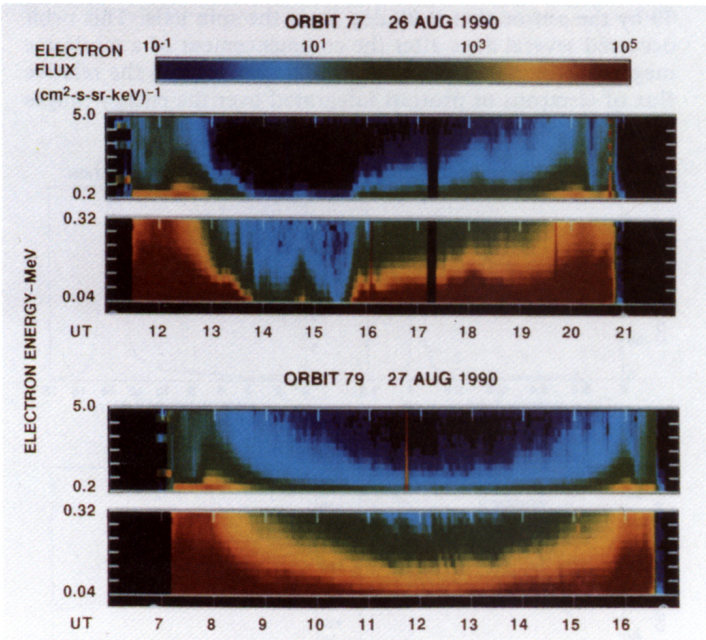

Fig. 5 Energy time spectrograms showing approximately spin-averaged fluxes of electrons during orbits 77 and 79.

indicated in the upper right-hand portion. The intensity is color coded according to the flux in 4-deg-wide pitch angle bins normalized to the average differential, directional flux measured during each sampling interval. A full energy and pitch angle distribution is obtained in 64 s in the normal SEP operating mode. The time axis in the plot is arranged with perigee near the beginning and end and apogee at the center. Note how the pitch angle coverage for this detector varies during the orbit. Depending on the orientation of the magnetic field, data from the other two sensors can extend the pitch angle coverage achievable with a single telescope. Evidence for both pancake and butterfly pitch angle distributions are apparent in this display.

Figure 5 shows energy time spectograms for electrons measured during orbits 77 and 79. The differential number fluxes are averaged over 32 s; because the satellite spin is about 29 s, these are approximately spin-averaged fluxes. The data for each orbit are shown in two panels corresponding to the low- and high-energy electron ranges. The large dropout in fluxes in the first half of the orbit is a result of the magnetic storm that commenced one orbit earlier. Two orbits later, the energetic particle fluxes have recovered. Just after 12 UT in orbit 79 there are three dispersive-like electron events possibly associated with substorm activity.

To obtain the differential particle flux from the SEP data, the counts in each sampling interval are divided by the product of the live time, the spectrometer geometric factor, the energy width of the channel for the particular mode, and the sensor particle detection efficiency for the channel. Pitch angle distributions for each sensor are calculated using the sensor look directions and the magnetic field direction determined from the onboard magnetometer.

Conclusions

The SEP experiment on CRRES operated almost continuously throughout the lifetime of the spacecraft. The data obtained in the CRRES orbit allows the computation of the particle distribution functions in phase space for energetic electrons and protons throughout the radiation belts. These distributions can be used for developing models of both the static and dynamic radiation belt populations. Preliminary work toward a dynamic model has been completed using SCATHA outer-belt electron distributions together with a general solution to a simple form of the simultaneous bimodal (radial and pitch-angle) diffusion equation.[10,11] The SEP data are especially suited for these types of studies because of the good angular resolution and extended pitch angle coverage provided by the three telescopes.

Acknowledgments

This work was primarily supported by the Office of Naval Research under Contract N00014-83-C-0476 and in part by the Lockheed Independent Research Program. The authors wish to thank J. C. Bakke, L. A. Hooker, and V. F. Waltz for their efforts in the design, development, and fabrication of this instrument. We also deeply appreciate the contributions provided at Lockheed by H. D. Voss and J. M. Quinn. Special appreciation goes to the Ball Aerospace Systems Division who built the CRRES satellite; to the USAF Space Test Program and the NASA Marshall Space Flight Center, who shared in the management of the project; to General Dynamics for the successful launch of Atlas-Centaur rocket; and to the USAF Consolidated Space Test Center, which operated the satellite.

References

[1]Baker, D. N., Blake, J. B., Klebesadel, R. W., and Higbie, P. R., "Highly Relativistic Electrons in the Earth's Outer Magnetosphere, 1. Lifetimes and Temporal History, 1979–1984," *Journal of Geophysical Research,* Vol. 91, No. A4, 1986, pp. 4265–4276.

[2]Baker, D. N., Blake, J. B., Callis, L. B., Belian, R. D., and Cayton, T. E., "Relativistic Electrons Near Geostationary Orbit: Evidence for Internal Magnetospheric Acceleration," *Geophysical Research Letters,* Vol. 16, No. 6, 1989, pp. 559–562.

[3]West, H. I., Jr., Buck, R. M., and Walton, J. R., "Electron Pitch Angle Distributions Throughout the Magnetosphere as Observed on Ogo 5," *Journal of Geophysical Research,* Vol. 78, No. 7, 1973, pp. 1064–1081.

[4]Reagan, J. B., Nightingale, R. W., Gaines, E. E., Imhof, W. L., and Stassinopoulos, E. G., "Outer Zone Energetic Electron Spectral Measurements," *Journal of Spacecraft and Rockets,* Vol. 18, No. 1, 1981, pp. 83–88.

[5]Teague, M. J., and Vette, J. I., "The Inner Zone Electron Model AE-5," National Space Science Data Center/World Data Center A for Rockets and Satellites, Rept. 72-10, Nov. 1972.

[6]Singley, G. W., and Vette, J. I., "The AE-4 Model of the Outer Radiation Zone Electron Environment," NSSDC 72-06, Aug. 1972.

[7]Stevens, J. R., and Vampola, A. L., "Description of the Space Test Program P78-2 Spacecraft and Payloads," Space and Missile Systems Organization, Air Force Systems Command, TR-78-24, Los

Angeles Air Force Station, Los Angeles, CA, Oct. 1978.

[8]Voss, H. D., Reagan, J. B., Imhof, W. L., Murray, D. O., Simpson, D. A., Cauffman, D. P., and Bakke, J. C., "Low Temperature Characteristics of Solid State Detectors for Energetic X-ray, Ion and Electron Spectrometers," *IEEE Transactions on Nuclear Science,* Vol. NS-29, No. 1, 1982, pp. 164–168.

[9]Voss, H. D., Bakke, J. C., and Roselle, S. N., "A Spacecraft Multichannel Analyzer for a Multidetector Solid State Detector Array," *IEEE Transactions on Nuclear Science,* Vol. NS-29, No. 1, 1982, pp. 173–177.

[10]Chiu, Y. T., Nightingale, R. W., and Rinaldi, M. A., "Simultaneous Radial and Pitch Angle Diffusion in the Outer Electron Radiation Belt," *Journal of Geophysical Research,* Vol. 93, No. A4, 1988, pp. 2619-2632.

[11]Chiu, Y. T., Rinaldi, M. A., and Nightingale, R. W., "Toward Dynamic Modeling of the Outer Electron Radiation Belt," *Journal of Geophysical Research,* Vol. 95, No. A8, 1990, pp. 12,069–12,074.

Low-Energy Ion Mass Spectrometer on CRRES

H. H. Collin,* J. M. Quinn,† G. R. Smith,‡
E. Hertzberg,§ and S. Roselle¶
Lockheed Palo Alto Research Laboratory,
Palo Alto, California 94034
and
S. J. Battel**
Battel Engineering, Tucson, Arizona 85718

Scientific Objectives

THE low-energy ion mass spectrometer (IMS-LO) (ONR-307-8-1,2) is part of the SPACERAD[1] payload on the CRRES[2]. IMS-LO is designed to measure the composition of plasmas that are the sources of radiation belt particles, and to provide data on the origin and acceleration processes of these plasmas. To achieve these objectives, the instrument measures energy and mass spectra covering the ranges of E/q = 0.11 – 35 keV/e and M/q from 1-32 amu/e with good coverage of pitch angles throughout the CRRES orbit.

Measurement Techniques

The IMS-LO-1,2 instruments on CRRES rely on essentially the same design that was successfully implemented with previous Lockheed instruments on SCATHA (launched January 1979) and S3-3 (launched July 1976). Improvements have been made with each version of the instrument in range of coverage, resolution, and operating flexibility.

IMS-LO-1 and IMS-LO-2 are identical instruments which are mounted on the aft surface of the spacecraft with their look directions at 135 and 105 deg to the spacecraft $+Z$ axis. In the spacecraft X-Y plane they are both at 45 deg from the $+X$ axis, clockwise viewing in the $+Z$ direction. CRRES spins about the Z axis with $+Z$ oriented sunward. The look directions of the instruments were chosen to maximize coverage of fluxes near the magnetic field line direction thoughout the mission. Each instrument performs ion-composition measurements in the energy per charge range 0.11–35 keV/e and the mass per charge range 1–32 amu/e. The energy range, which is covered by 45 energy steps, is broken into three contiguous parts (j = 0,2), each consisting of 15 energy steps (i = 0,14). The mean energy per charge E_{ij} of ions on the ith step of the jth part is given by

$$E_{ij}\ (\text{keV}) = 0.109 \times (1.14008)^{(i+15j)} \qquad (1)$$

The three parts of the energy coverage are sampled in parallel by three separate analyzer and sensor units ("heads"). At the completion of each 15-step sequence, the background counting rate is measured for each sensor head. The mass range (1–32 amu/e) is covered by 32 steps. Alternatively, the spectrometer can be commanded to a heavy-ion mode as described in the section below on operating modes and control. In addition to ion measurements, each of the two instruments monitors the background electron flux at four fixed energies. The electron channels are described in a separate section below.

Ion Optics

Each of the IMS-LO mass spectrometers consists of three analyzer heads which measure ions in a different portion of the E/q range from 0.11–35 keV/e. One of the analyzer heads is illustrated in Fig 1. Each analyzer consists of four sections: a collimator, a velocity filter, an energy analyzer, and a channel electron multiplier detector.

Ions enter the instrument through the collimator that provides an acceptance cone of approximately 5-deg full width. Following collimation, the ions enter the crossed electric and magnetic field velocity filter (Wien filter), which acts as the mass analyzer (MA). Its magnetic field is fixed while the crossed electric field is varied according to the value of E/q and M/q being sampled. The fields are oriented so that the electric and magnetic forces on an ion are in opposition, and

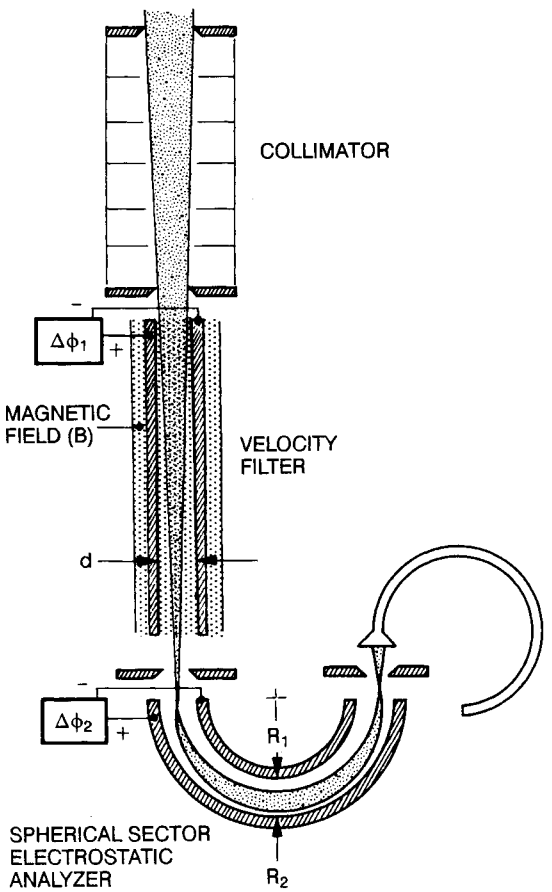

Fig. 1 Ion mass and energy analysis optics for the low energy ion mass spectrometer.

Received June 13, 1991; revision received Aug. 8, 1991; accepted for publication Aug. 9, 1991.

*Research Scientist.
†Staff Scientist.
‡Scientist.
§Staff Engineer
¶Senior Engineer.
**Consultant, 7601 N Calle Sin Envida #62. Member AIAA.